

Material Properties of Hagfish Skin, with Insights into Knotting Behaviors

ANDREW J. CLARK^{1,*}, CALLIE H. CRAWFORD¹, BROOKE D. KING¹,
ANDREW M. DEMAS¹, AND THEODORE A. UYENO²

¹*Department of Biology, College of Charleston, 66 George Street, Charleston, South Carolina 29424; and*

²*Department of Biology, Valdosta State University, 1500 N. Patterson Street, Valdosta, Georgia 31698*

Abstract. Hagfishes (Myxiniidae) often integrate whole-body knotting movements with jawless biting motions when reducing large marine carcasses to ingestible items. Adaptations for these behaviors include complex arrangements of axial muscles and flexible, elongate bodies without vertebrae. Between the axial muscles and the hagfish skin is a large, blood-filled subcutaneous sinus devoid of the intricate, myoseptal tendon networks characteristic of the taut skins of other fishes. We propose that the loose-fitting skin of the hagfish facilitates the formation and manipulation of body knots, even if it is of little functional significance to steady swimming. Hagfish skin is a relatively thick, anisotropic, multilayered composite material comprising a superficial, thin, and slimy epidermis, a middle dermal layer densely packed with fibrous tissues, and a deep subdermal layer comprised of adipose tissue. Hagfish skin is stiffer when pulled longitudinally than circumferentially. Stress-strain data from uniaxial tensile tests show that hagfish skins are comparable in tensile strength and stiffness to the taut skins of elongate fishes that do not engage in knotting behaviors (*e.g.*, sea lamprey and penpoint gunnel). Sheath-core-constructed ropes, which serve as more accurate models for hagfish bodies, demonstrate that loose skin (extra sheathing) enhances flexibility of the body (rope). Along with a loose-fitting skin, the morphologies of hagfish skin parallel those of moray eels, which are also known for generating and manipulating figure-eight-style body knots when struggling with prey.

Introduction

Hagfishes (myxiniid fishes) use a remarkable feeding system devoid of jaws and rigid support tissues to deliver forceful and dynamic biting movements (Clark and Summers, 2007). This system can be used to its best effect when coupled with whole-body knotting (Clark and Summers, 2012; Uyeno and Clark, 2015). When the hagfish handles large food items (*e.g.*, whole fish carcasses with intact, puncture-resistant skins), a knot forms in the posterior body, and then slides towards the head so that it can be pressed against the food surface. The body knot then makes a stable platform that effectively antagonizes the toothplate movements when it is in contact with the food item (Uyeno and Clark, 2015). In addition to feeding behaviors, the knotting movements of hagfish can be elicited when the animals are discarding excess slime from their body surfaces and when attempting to evade predators (Jensen, 1966). In all cases, hagfish knotting is executed with an impressive combination of speed, agility, and precision; however, these behaviors are rarely observed in extant fishes, including elongate, gape-limited species. The formation and manipulation of body knots requires coordinated bending and twisting movements, which, we theorize, are facilitated in hagfish by the presence of a flexible, elongate body devoid of vertebrae, a relatively complex arrangement of axial musculature, and loose skin.

Other than a dorsal median septum and some connective tissue fiber linkages along the ventral midline (Fig. 1A), hagfishes lack fibrous myoseptal-skin connections (Vogel and Gemballa, 2000), giving their skin a loose-fitting appearance. The slackness is more visible in examples of *Eptatretus stoutii* and less so in the skins of *Myxine glutinosa*, and while this might imply some diversity in skin tautness across hagfish species, the skins of all hagfish are

Received 16 June 2015; Accepted 13 May 2016.

* To whom correspondence should be received. E-mail: clarkaj@cofc.edu

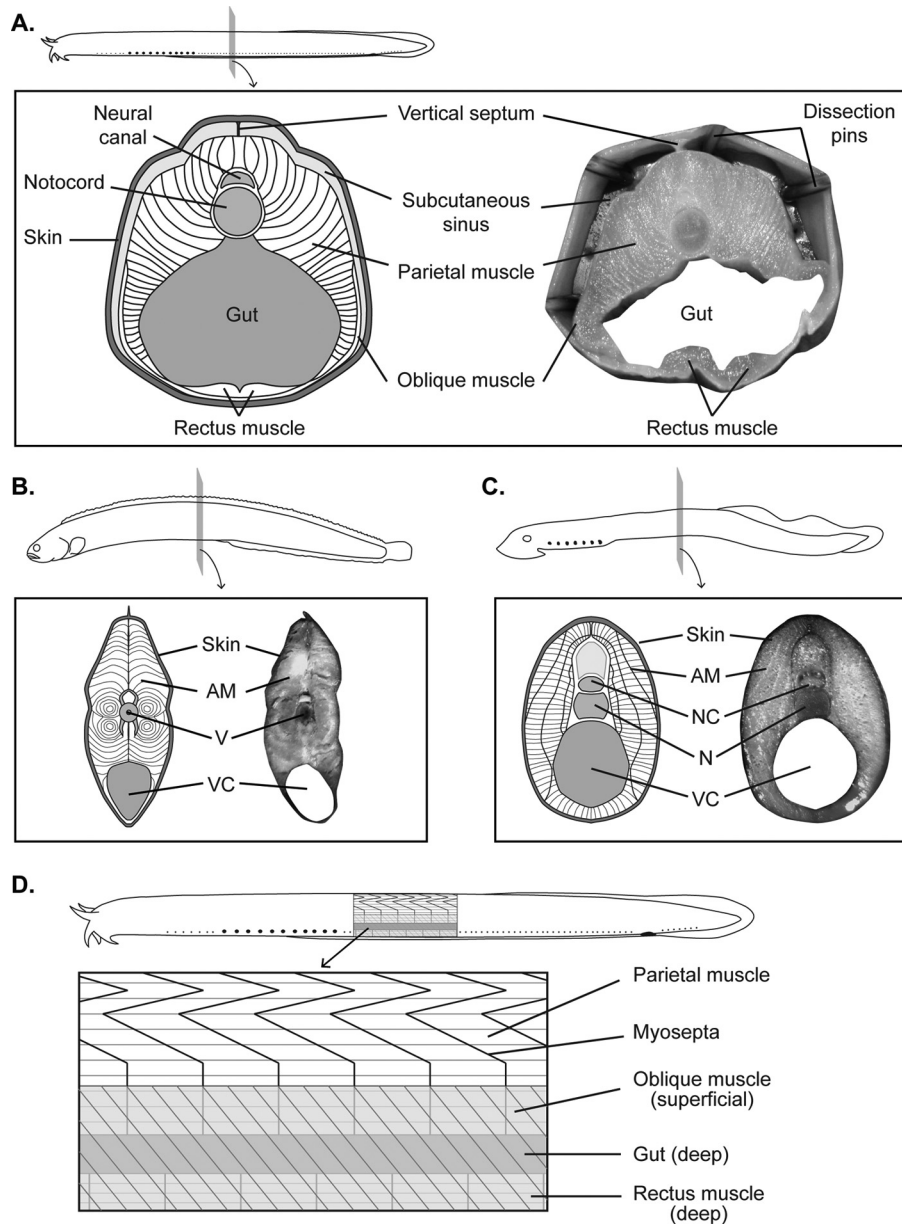


Figure 1. General axial morphology of three species of elongate fishes examined in the present study. (A) Lengthwise sketch (top) and (inset) diagram and photograph of cross-sectional views of the axial anatomy of *Eptatretus stoutii* at approximately 50% total length (TL). *Inset*: Note the overlap between different muscle groups and the loose fit of the integument. In the photograph, the skin along the dorsal and lateral margins of the transverse section has been retracted with dissection pins to show the subcutaneous sinus. (B) (C) Lengthwise sketches (top) and (insets) left lateral diagrams and photographs of penpoint gunnel *Apodichthys flavidus* (B) and sea lamprey *Petromyzon marinus* (C); the transverse sections are at approximately 50% TL. (D) Diagram showing a left lateral view of a Pacific hagfish *Eptatretus stoutii*, with body core musculature at about 50% TL highlighted to show the three muscle groups of myxiniid fishes: the parietal muscle, oblique muscle, and rectus muscle. AM, axial muscles; N, notocord; NC, neural canal; V, vertebrae; VC, visceral canal.

substantially decoupled from the body core (A. J. Clark, pers. obs.). This morphology in hagfishes is a clear contrast to the taut, close-fitting skins of other fishes (lampreys and cartilaginous and bony fishes) that possess firm myoseptal fiber attachments between the axial muscles and skin (Fig.

1B, C). Between the innermost surface of the hagfish skin and axial musculature is a considerably large subcutaneous sinus (Fig. 1A), which contains approximately 30% of the total blood volume in an individual (Forster, 1998) and probably explains the proportionately high blood volume in

hagfishes compared with other fishes (McDonald *et al.*, 1991). Unlike the body core musculature of other basal chordates and fishes, the body core musculature of myxiniid fishes is comprised of three groups (Fig. 1D): the segmented parietal and the rectus muscles, both of which are overlapped by the superficial, non-segmented oblique muscles (Cole, 1907; Jansen and Andersen, 1963; Vogel and Gemballa, 2000). This arrangement and orientation of muscle fibers in the body core generate the forces that bend and twist a hagfish as it creates a body knot. In most taut-skinned fishes, the body core musculature is made up of segmented and serially arranged, cone-shaped myomeres divided into epaxial and hypaxial muscle groups by a horizontal septum (Liem *et al.*, 2001). Myoseptal connective tissue sheets attach adjacent blocks of muscle to one another, and myoseptal-skin connections affix the skin's dermis, or *stratum compactum*, to the body core musculature (Gemballa and Vogel, 2002). The taut skins of most fishes should be functionally important in aquatic locomotion, because these firm myoseptal-skin connections can transmit the tension produced by the axial muscles to the dermis (Gemballa and Vogel, 2002; Gemballa and Treiber, 2003; Summers and Long, 2006).

Relative to the longitudinal axis, the taut skins of cartilaginous (*e.g.*, Motta, 1977) and bony fishes (*e.g.*, Fujii, 1968) are reinforced with left and right cross-helical arrangements of collagen fibers, allowing the skin to form a rigid framework to support internal tissues yet remain flexible enough to permit the whole-body deformations required for swimming (Hebrank and Hebrank, 1986). This particular orientation of connective tissue aids in retaining an animal's cross-sectional area as its body core pressurizes; it also prevents the bending body from kinking (Clark and Coway, 1958). The tight-fitting skins of most fishes are reinforced with cross-helically arranged, tension-resistant fibers that function well in limiting dangerous axial strains, and which, in some species, may function like "exotendons" by effectively transmitting forces from the body core to the environment (Wainwright *et al.*, 1978; Hebrank, 1980). However, thrust generation pathways from body core muscles to water vary across fish species (Long *et al.*, 1996, 2002a; Müller and Van Leeuwen, 2006). Additional studies have shown that some fish skins do not function like external tendons (Hebrank and Hebrank, 1986; Summers and Long, 2006). In all cases, however, taut body coverings are helpful in preventing unwanted shape changes of the body core and in minimizing drag during swimming. In contrast, structures with floppy coverings experience more drag (Vogel, 1994). Since it is the skin that interfaces with the aquatic medium, the absence of myoseptal-skin connections in hagfishes likely results in an indirect and reduced transmission of muscle-generated force to the skin and, ultimately, to the water (Vogel and Gemballa, 2000). Slack skin is problematic for generating thrust because the forces pro-

duced by the body core muscles will tend to shear relative to the inner surface of the skin instead of being directly transmitted to the dermis *via* fibrous tissue. Furthermore, the skins of the Atlantic hagfish *Myxine glutinosa* have minimal influence on whole-body flexural stiffness during steady swimming movements across various body speeds (Long *et al.*, 2002b).

Hagfish skin is a poor exotendon, and is functionally insignificant at biologically relevant, steady swimming speeds. However, the loose connection between the skin and the underlying axial muscles may present functional opportunities for knotting, for example, by enhancing flexibility of the predominately decoupled body core and becoming a deformation-resistant covering when the body core undergoes extremely large axial strains characteristic to knotting. The mechanical behavior of fish skin is worthy of attention not only because the skin interfaces directly with the aquatic medium, but because its location farthest from the animal's neutral-bending axis within the vertebral column means that it experiences the largest stresses and strains during swimming (*e.g.*, cyclic tension, compression of convex and concave sides of the body) (Long *et al.*, 1996). Material properties of the skins of cartilaginous (*e.g.*, Naresh *et al.*, 1997) and bony fishes (*e.g.*, Hebrank, 1980; Hebrank and Hebrank, 1986; Brainerd, 1994) have been measured; however, data sets from testing on jawless fish skins have yet to be published. Given the extraordinary axial morphology and movements of hagfishes, the probable but unresolved functional link between fish integument and locomotion, and the overall paucity of data, the skins of myxiniid fishes make a fascinating and convenient system for investigating morphological and mechanical characteristics associated with whole-body knotting movements.

Steady swimming in fishes, primarily in the form of lateral undulation, is characterized by the cyclic bending movements of the body produced by axial muscle forces transmitted to the vertebral column. Bending of the body's longitudinal axis, coupled with elaborate myoseptal-skin connections, produce a suite of tensile stresses and strains that the skin must accommodate to permit adequate locomotion. Studies have shown that the taut skins of other fishes are more resistant to tensile strains directed circumferentially than to those directed longitudinally (Hebrank, 1980; Hebrank and Hebrank, 1986; Naresh *et al.*, 1997). However, for the hagfish to create a successful knot, the body core muscles must produce both bending and torsional movements. For these purposes, hagfish could benefit from integument that is mechanically less resistant to tensile strains directed circumferentially than the taut skin of other fishes.

In this study, we gathered data sets from uniaxial tensile testing on myxiniid skins that were strained in longitudinal

and circumferential body axes to assess fundamental material properties (tensile strength and stiffness along longitudinal and circumferential axes). We then qualitatively compared these data with similar information gathered from other species. We measured strength and stiffness in the skins of the Pacific hagfish *Eptatretus stoutii*, and, for comparison, we collected similar data sets from the skins of the penpoint gunnel *Apodichthys flavidus* (Fig. 1B) and the sea lamprey *Petromyzon marinus* (Fig. 1C). These elongate fishes were chosen because they possess taut skins and do not perform knotting. We obtained these data to determine 1) if the loose-fitting skins of hagfish, without myoseptal-skin connections, are weaker and/or less stiff than the taut skins of other fish species; 2) if the skins of hagfish, which undergo torsion during knotting, are more compliant in the circumferential axis than the skins of other fishes; and 3) whether the material properties of hagfish skins vary with respect to location on the body. Using tensile testing, gross dissection, histology, and simple modeling, we aimed to identify features of hagfish integument that could aid in the production and manipulation of body knots in an attempt to understand why these fishes possess loose-fitting skins that are of little, if any, benefit to thrust production and steady swimming.

Materials and Methods

Specimens

Specimens of Pacific hagfish *Eptatretus stoutii* (Lockington, 1878) were collected from about one mile off the coast of San Pedro, California, in July 2011, by the California Fish and Game Commission. Hagfish specimens were euthanized with an overdose of tricaine methanesulfonate (MS-222), then transferred to a -30°C freezer. Frozen specimens were shipped to the College of Charleston, South Carolina, where they remained frozen at approximately -30°C until experimentation. All animals were thawed once before skin-sample preparation and mechanical testing. Skin samples from 5 specimens of *E. stoutii*, whose total length (TL) ranged between 38.0–47.0 cm, were tested in Charleston, South Carolina, in August 2011.

Newly metamorphosed adult specimens of sea lamprey *Petromyzon marinus* Linnaeus, 1758 were collected from Branch Brook near Kennebunk, Maine, in January 2012, by Acme Lamprey Company (Harrison, ME). Lamprey specimens were euthanized with an overdose of MS-222, then frozen at approximately -30°C . The frozen lamprey specimens were shipped to the College of Charleston, then thawed once prior to sample preparation and experimentation. Skin samples from 5 specimens of *P. marinus* (TL 17.0–18.0 cm) were tested in Charleston in March 2012.

Specimens of penpoint gunnel *Apodichthys flavidus* Girard, 1854 were collected by seine fishing at Jackson Beach, San Juan Island, Washington, in July 2012. *A. flavidus*

specimens were housed in sea tables connected to a flow-through seawater system at the University of Washington's Friday Harbor Laboratories (Friday Harbor, WA). Before dissection of skin and sample preparation, *A. flavidus* specimens were euthanized with an overdose of MS-222. The methods of collection and handling of living specimens of *A. flavidus* were approved by the University of Washington's Institutional Animal Care and Use Committee (Protocol no. 4238-03). Skin samples of *A. flavidus* were collected from 4 specimens (TL 28.7–35.6 cm) and tested in Friday Harbor, WA, in July 2012.

Sample preparation

Sixteen skin samples were fabricated from each specimen of *Eptatretus stoutii* and *Apodichthys flavidus*; eight anterior and eight posterior samples were collected from the left and right sides of each animal (Fig. 2A). Anterior and posterior skin samples were created from larger rectangular portions of skin removed from the left and right sides of each animal at about the 25% and 75% landmarks of TL, respectively (Fig. 2A). Each rectangle was divided into four samples: two samples to be strained along the animal's longitudinal axis, and two samples to be strained in the circumferential (or hoop) direction, orthogonal to the longitudinal axis (Fig. 2B). One skin sample from each pair of samples was rectangular (17.0 mm long \times 6.0 mm wide) to measure Young's modulus (stiffness); the other sample from each pair was "dumbbell"-shaped (17.0 mm long \times 2.0 mm wide in the narrow-waisted region of the sample's mid-length) to measure peak stress (strength) (Fig. 2B, C). The purpose of fabricating dumbbell-shaped skin samples was to produce a known region on the sample where tensile stress contours were concentrated and failure must occur, that is, at the region where the cross-sectional area (CSA) is smallest. In our study, the narrowest (smallest CSA) section of the dumbbell-shaped samples was prepared by cutting out triangular notches on each side of the rectangular samples (Fig. 2B, C).

We used triangle-notched samples instead of the conventional semi-oval notches, because traditional sample shapes were difficult to fabricate in hagfish and gunnel skins; breakage also occurred in unexpected areas. Even though the sample shapes used here were unorthodox, the triangular notches accomplished the same purpose as traditional notches: they established a region of the skin sample where failure must occur (*i.e.*, where the sample's CSA was smallest and the stress contours were most concentrated). After fabrication and dimensional measurements were recorded, samples were kept moist in KimWipes (Kimberly-Clark, Irving, TX) soaked in seawater (full seawater at 33‰ for *E. stoutii* samples and one-third seawater at 11‰ for *A. flavidus* samples).

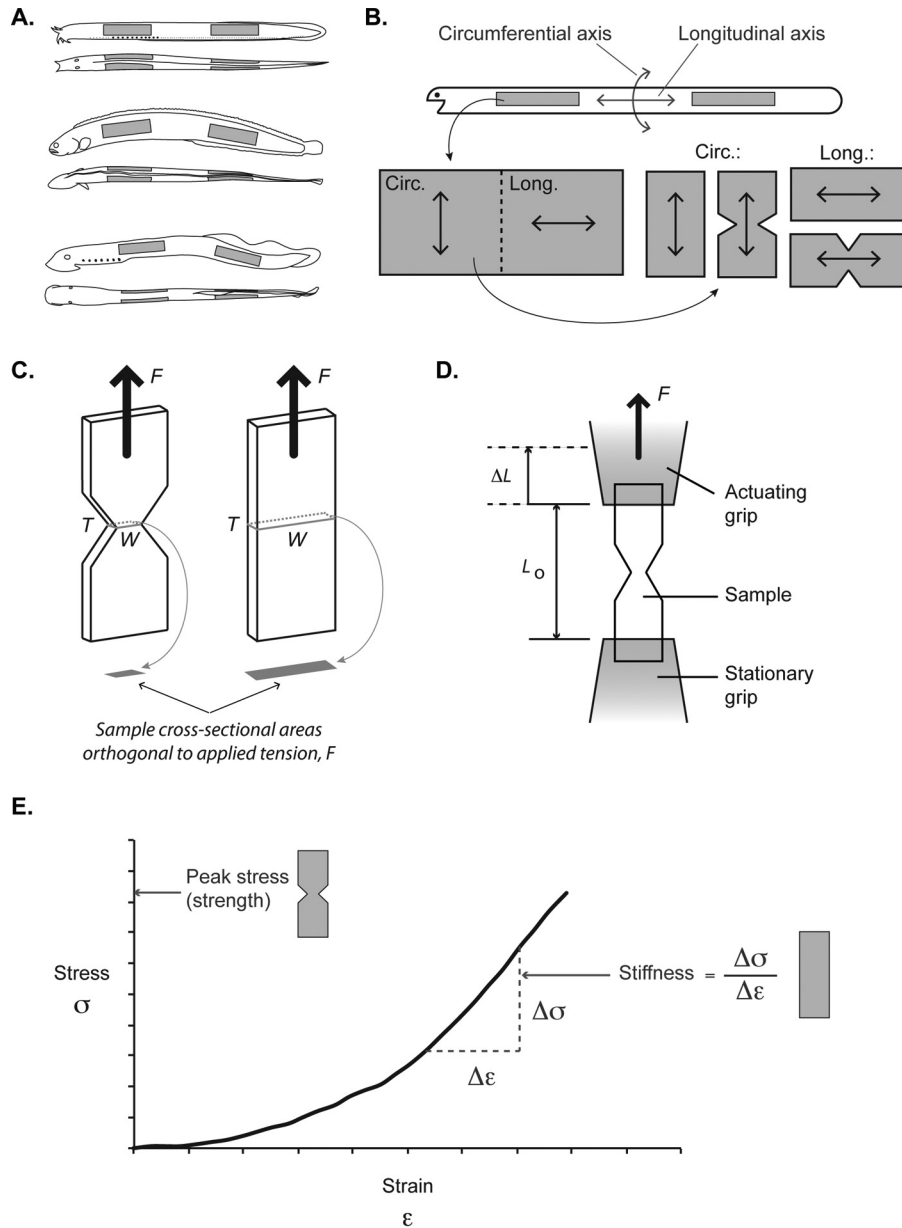


Figure 2. Methodologies used for collecting, fabricating, testing, and analyzing skin samples. (A) Diagrams of left lateral and dorsal views of the three species of elongate fishes examined in the present study. Gray rectangles in each image represent locations of skin samples collected for tensile tests. (B) Diagrams of methods used for collecting and fabricating skin samples for tensile testing along circumferential (Circ.) and longitudinal (Long.) axes in the head and tail regions. Strength was measured from tensile tests performed on dumbbell-shaped samples; stiffness was measured from tensile tests performed on rectangular samples. A dumbbell-shaped sample was prepared by cutting out triangular notches from each side of a sample originally shaped as a rectangle. (C) Methods used for measuring test sample dimensions (width (W); thickness (T)) from rectangles and dumbbells. Note the proportionately smaller cross-sectional area in the dumbbell-shaped samples. (D) Schematic diagram of a uniaxial tensile test to failure conducted on a dumbbell-shaped sample, with the methods for measuring the variables for strain data (original length (L_0); change in length (ΔL)). (E) Graph of methods used for measuring strength and stiffness from stress-strain curves. Note that stress-strain data from rectangular samples were used for measuring stiffness, while data gathered from dumbbell-shaped samples were used for measuring strength.

Eight skin samples were fabricated from each *Petromyzon marinus* specimen, with four samples collected from the anterior left and right sides of the body, and four samples

collected from the posterior left and right sides. Anterior samples were created from rectangular portions of skin removed from approximately the 30%–35% points of the

animal's TL, immediately posterior to the gill openings, while posterior samples were made from rectangular samples collected from the 75% point of TL (Fig. 2A). Each rectangle was divided into two smaller rectangles, 15.0 mm long \times 8.0 mm wide, which were to be strained along the animal's longitudinal axis. Lamprey skin samples shaped as dumbbells and samples to be strained circumferentially were difficult to form due to the small size of the specimens; therefore, only Young's modulus from skin samples strained longitudinally was measured in this study. Before mechanical testing, lamprey skin samples were measured and retained in KimWipes soaked in Ringer's solution (101 mmol l⁻¹ NaCl, 3.3 mmol l⁻¹ KCl, 2.5 mmol l⁻¹ CaCl₂, 2.5 mmol l⁻¹ NaHCO₃, 1.2 mmol l⁻¹ KH₂PO₄, and 1.3 mmol l⁻¹ MgSO₄) (Urist, 1963; Evans and Harrie, 2001).

Mechanical testing

The present study represents a first approximation of the mechanics of myxinid integument, in which we subjected all fabricated skin samples from all study species to quasi-static, uniaxial tensile tests to failure. Non-destructive testing approaches and analyses of loading and unloading phases of stress-strain curves were not planned for this study. At the College of Charleston, an IMADA EMX-275 Motorized Vertical Test Stand (Imada, Inc., Northbrook, IL) was used to conduct tensile tests on skin samples from the five *E. stoutii* and five *P. marinus* specimens. At Friday Harbor Laboratories (FHL), an MTS Synergie vertical testing stand (MTS Systems Corp., Eden Prairie, MN) was used for testing skin samples of four *A. flavidus* specimens.

To prevent the clamped skins from slipping during the tensile tests, small squares of 80-grit sandpaper were folded over the portion of sample to be clamped with standard serrated grips. All skin samples were strained at a rate of 25 mm/min; force and extension data were recorded at 10.0 Hz with the MTS Synergie, and at 2.0 Hz with the IMADA EMX-275. Skin samples of four additional *Eptatretus stoutii* tested with the MTS system (and also strained at 25 mm/min) yielded results similar to those for the five specimens tested with the IMADA system, suggesting that the different sampling rates from these two testing systems were not problematic. Stress (σ) and strain (ϵ) were derived from measurements of force (F) and extension (L). Stress was calculated as:

$$\sigma = \frac{F}{CSA}$$

The cross-sectional area (CSA) of each sample, which was the area orthogonal to the applied tensile force (F), was calculated as the product of sample width and thickness. Sample dimensions, width, and thickness were measured with digital calipers (\pm 0.01 mm). Strain was calculated as:

$$\epsilon = \frac{\Delta L}{L_0}$$

where ΔL represents the change in length during the tensile test, and the initial sample length prior to testing (L_0) equals the grip separation (Fig. 2D). All skin samples exhibited J-shaped stress-strain curves comprising a shallow-sloped, curvy toe region at lower strains, followed by a steeper-sloped linear region at greater strains (Fig. 2E). Peak stress (strength, or σ_{MAX}) was defined as the maximum applied stress prior to failure; Young's Modulus (stiffness, or E) was defined as the ratio of stress to strain in the linear region following the curvy toe region of the stress strain curve (Fig. 2E).

Morphology of hagfish skin

Our initial examinations of hagfish skin samples revealed that thickness (*e.g.*, when viewed along a sliced edge with magnifying glasses) was largely comprised of a fibrous tissue layer and a fatty tissue layer. For further examination of the morphology of hagfish skin, we photographed the sliced edges of each test sample positioned under a stereomicroscope prior to testing. We also used untested skin samples collected from each hagfish specimen at the head region (dorsal surface posterior to the eye spots), the lateral surfaces at the tail region, and the ventral surface (beneath the feeding apparatus, anterior to gill pouches) for histological examination. Samples were fixed in 10%-buffered formalin, dehydrated with ethanol, embedded in paraffin, and sectioned at 5 μ m. Sections were made along the longitudinal plane of the animal and stained with hematoxylin and eosin.

Data analysis

Data on strength and stiffness as measured from the hagfish and gunnels were organized by anatomical location (head or tail) and the direction of force (longitudinal or circumferential). Within each species, we used paired sample *t*-tests with Bonferroni corrections to compare the mean data (strength and stiffness) between skin samples measured from the left and right sides of the body, the head and tail regions, and the longitudinal and circumferential directions. We used $P < 0.016$ as the criterion for significance for all paired *t*-tests involving data from hagfish and gunnels. This adjusted alpha equaled the initial alpha ($\alpha = 0.05$) divided by three, representing the number of hypotheses tested (left side *vs.* right side, head region *vs.* tail region, and longitudinal *vs.* circumferential direction). Data sets gathered from sea lamprey were organized by anatomical location (head or tail); paired sample *t*-tests with Bonferroni corrections were used to compare data (stiffness in the longitudinal direction) between the left and right sides and between the head and tail regions. We used $P < 0.025$ as the criterion for significance in all paired *t*-tests involving data from lamprey, which equaled the initial alpha ($\alpha = 0.05$) divided by two,

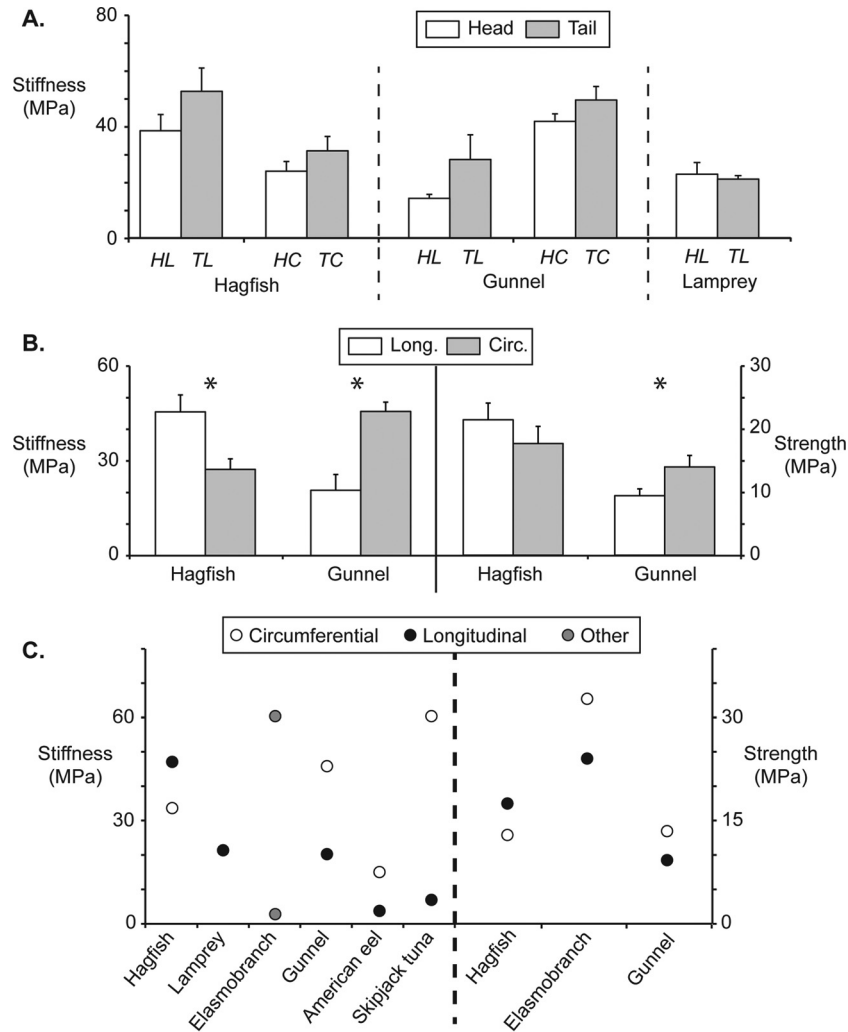


Figure 3. Material properties of fish skins. (A) Stiffness data gathered from skins of the Pacific hagfish, penpoint gunnel, and sea lamprey. Data are organized by their location (head (H) or tail (T)) and the direction of the tensile tests (longitudinal (L) or circumferential (C)). (B) Stiffness (left) and strength (right) of hagfish and gunnel skin samples pulled uniaxially in longitudinal (Long.) or circumferential (Circ.) body axes. Note the anisotropy in the stiffness of both types of skins. (C) Data sets for stiffness (left) and strength (right) from the present study, plotted with published data gathered from studies on elasmobranchs (Naresh *et al.*, 1997), American eels (Hebrank, 1980), and skipjack tuna (Hebrank and Hebrank, 1986). (A) and (B) present mean values \pm SEM; significant differences between means are indicated with asterisks.

representing the number of hypotheses tested (left side vs. right side and head region vs. tail region).

Results

Mechanical testing

Mean strength and mean stiffness from hagfish and gunnel skin samples, which were organized by body location and direction of applied tensile load, did not differ between the animals' left and right sides. Left- and right-side data sets from each animal were subsequently averaged for comparisons between the mean strength and stiffness with respect to location and direction (Fig. 3A). The skin samples

collected from the cranial (at approximately 25% TL) and caudal regions (at about 75% TL) of the hagfish and gunnels were also similar in strength and stiffness (Table 1). Direction-specific data from the head and tail were then pooled for subsequent comparisons between the longitudinal and circumferential directions (Table 2).

The skins of the Pacific hagfish and penpoint gunnels were anisotropic, meaning, the material properties of stiffness (E) and strength varied significantly with the direction of the applied load (Fig. 3B). The mean stiffness (\pm SEM) of hagfish skins pulled longitudinally ($E = 45.5 \pm 5.35$ MPa) was significantly greater than—about twice that—of

Table 1

Material properties of skin samples excised from the head and tail regions of Pacific hagfish, penpoint gunnels, and sea lamprey

Location and body axis	Pacific hagfish <i>Eptatretus stoutii</i>	
	Stiffness (MPa)	Strength (MPa)
Head (Long.)	38.5 ± 5.82	19.3 ± 2.07
Tail (Long.)	52.6 ± 8.36	25.5 ± 3.91
Paired <i>t</i> -test	$t_4 = 2.03; P = 0.112$	$t_4 = 1.87; P = 0.135$
Head (Circ.)	24.0 ± 3.48	14.1 ± 1.92
Tail (Circ.)	31.3 ± 5.18	21.2 ± 4.81
Paired <i>t</i> -test	$t_4 = 1.92; P = 0.128$	$t_4 = 2.17; P = 0.100$
Location and body axis	Penpoint gunnel <i>Apodichthys flavidus</i>	
	Stiffness (MPa)	Strength (MPa)
Head (Long.)	13.3 ± 1.30	7.60 ± 1.68
Tail (Long.)	28.2 ± 8.85	11.2 ± 0.765
Paired <i>t</i> -test	$t_3 = 1.70; P = 0.188$	$t_3 = 2.10; P = 0.127$
Head (Circ.)	41.8 ± 2.67	11.5 ± 1.94
Tail (Circ.)	49.5 ± 4.85	13.0 ± 1.21
Paired <i>t</i> -test	$t_3 = 2.35; P = 0.100$	$t_3 = 0.539; P = 0.100$
Location and body axis	Sea lamprey <i>Petromyzon marinus</i> *	
	Stiffness (MPa)	
Head (Long.)	22.8 ± 9.37	
Tail (Long.)	21.1 ± 2.82	
Paired <i>t</i> -test	$t_4 = 0.450; P = 0.678$	

Strength and stiffness (both expressed as means ± SEM) were measured from samples of hagfish and gunnel skins strained along longitudinal (Long.) and circumferential (Circ.) body axes. Mean stiffness measurements from newly metamorphosed sea lamprey skin samples strained along the longitudinal axis are included. Results from paired *t*-tests comparing head and tail means of each species appear under their respective data sets.

*Stiffness data along the circumferential axis, and strength data along both axes, from newly metamorphosed sea lamprey were excluded from this study (see text for details).

skins pulled circumferentially ($E = 26.65 \pm 2.71$ MPa) (paired *t*-test: $t_9 = 3.22; P = 0.010$). However, the hagfish skin samples that were strained longitudinally and circumferentially were similar in strength ($\sigma_{MAX} = 20$ MPa; paired *t*-test: $t_9 = 2.27; P = 0.049$). Gunnel skin samples pulled circumferentially ($E = 45.75 \pm 2.94$ MPa) were significantly stiffer than samples pulled longitudinally ($E = 20.75 \pm 5.01$ MPa; paired *t*-test: $t_7 = 6.64; P = 0.00029$). Skin samples from the gunnels were also significantly stronger ($\sigma_{MAX} = 14.05 \pm 1.80$ MPa) in the circumferential axis than in the longitudinal axis ($\sigma_{MAX} = 9.45 \pm 1.09$ MPa; paired *t*-test: $t_7 = 3.85; P = 0.0063$).

As with the hagfish and gunnel skins, lamprey skin samples showed no difference in stiffness in the longitudinal axis between the left and right sides of the body. These data were then averaged per individual for comparison of stiffness between the cranial and caudal regions (Fig. 3A; Table

1). In the newly metamorphosed sea lamprey, mean skin stiffness at the head region ($E = 22.8 \pm 4.19$ MPa) was similar to that of the tail region ($E = 21.1 \pm 2.82$ MPa; paired *t*-test: $t_4 = 0.450; P = 0.676$). For qualitative comparisons, the mean data from Pacific hagfish, sea lamprey, and penpoint gunnels were plotted, with some published values, for tensile strength and stiffness of other fish skins (Fig. 3C).

Morphology

The loose-fitting skins of living, recently euthanized, thawed specimens of Pacific hagfish are slimy and oily, which makes them considerably difficult to handle when conducting simple mechanical tests as described here. In all parts of the hagfish body, the skin is comprised of three distinct tissue layers: the epidermis, dermis, and subdermis (Fig. 4A, B). The thinnest and outermost layer, the epidermis, was identifiable only in photographs of stained histological sections of the skin. Positioned deep to the thin epidermis (< 20 μm in thickness) are the thicker dermal and subdermal tissue layers. Photographs of samples under both stereomicroscope and light microscope demonstrate the general morphology of these two distinct layers (Fig. 4A, B). The fibrous dermis of the hagfish (ranging from 105–205 μm in thickness) makes up 20%–30% of the total skin thickness, and is composed of densely packed connective tissues arranged in a plywood-like pattern (Fig. 4B). The thicker, softer fatty subdermis (326–727 μm in thickness) can account for up to 75% of total skin thickness, and is composed of large, globular adipose cells (Fig. 4A, B).

Table 2

Anisotropy in the skins of Pacific hagfish and penpoint gunnels

Body axis	Pacific hagfish <i>Eptatretus stoutii</i>	
	Stiffness (MPa)	Strength (MPa)
Longitudinal	45.5 ± 5.35	21.45 ± 2.65
Circumferential	26.7 ± 2.71	17.6 ± 2.71
Paired <i>t</i> -test	$t_9 = 3.22; P = \mathbf{0.010}$	$t_9 = 2.27; P = 0.049$
Body axis	Penpoint gunnel <i>Apodichthys flavidus</i>	
	Stiffness (MPa)	Strength (MPa)
Longitudinal	20.6 ± 5.01	9.45 ± 1.09
Circumferential	45.8 ± 2.94	14.05 ± 1.80
Paired <i>t</i> -test	$t_7 = 6.64; P = \mathbf{0.00029}$	$t_7 = 3.85; P = \mathbf{0.0063}$

Within each species, strength and stiffness (both expressed as means ± SEM) were compared between samples strained in the longitudinal and circumferential axes. Results from paired *t*-tests with Bonferroni adjustments used for comparing body axes within each species are included under their respective data sets. Significant differences are indicated in bold (see text for details on the criteria for meeting significance).

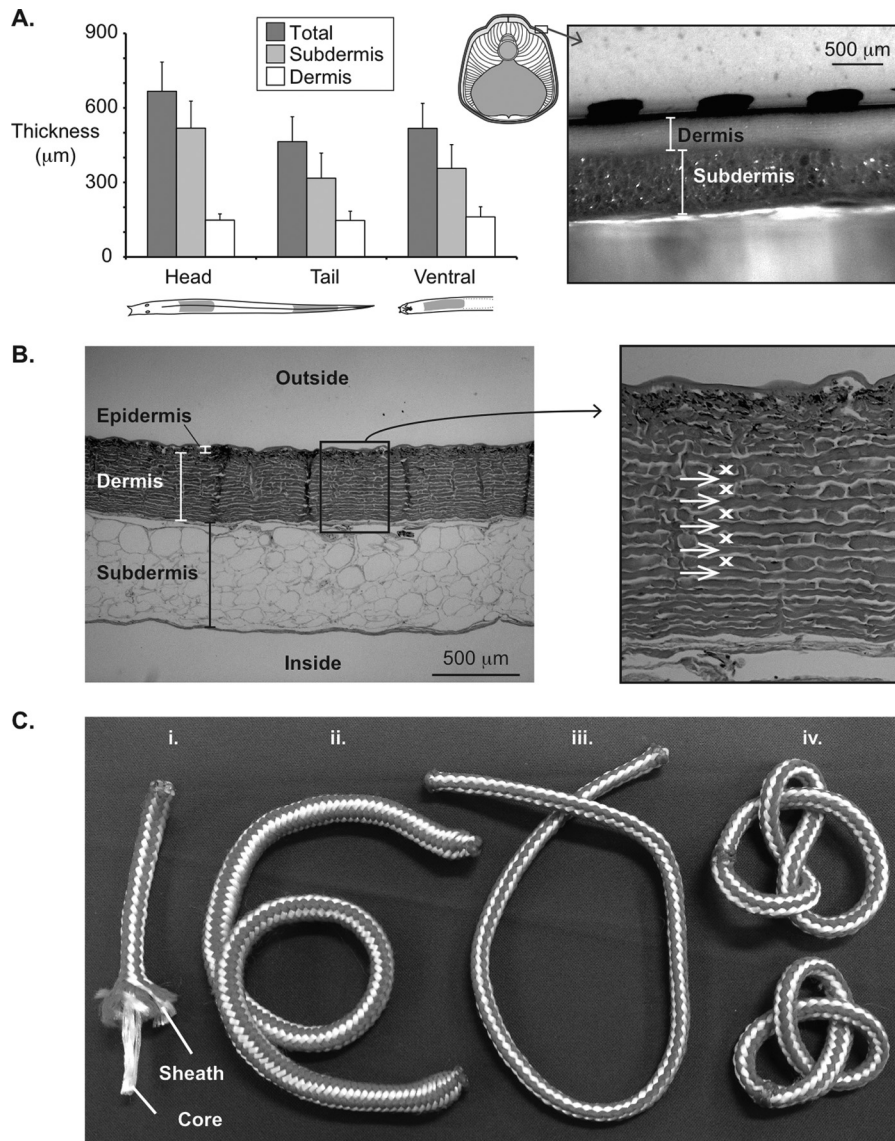


Figure 4. Morphology of Pacific hagfish skin and rope models for hagfish bodies. (A) *Left:* graph showing total thickness of the skin in the head, tail, and ventral body regions of Pacific hagfish, with relative percentages of the dermis and subdermis indicated for each body region. *Right:* photograph of a stereomicroscopic view of a hagfish skin sample in the transverse plane, showing the dermal and subdermal layers. (B) Photographs taken from light microscopic (4× magnification and 10× magnification in the left and right photos, respectively) views of a transverse section of hagfish skin stained with hematoxylin and eosin. Note the plywood-like arrangement of adjacent fibrous layers in the dermis; small white arrows indicate layers with fibers running continuously from left to right; white “x” markings point to fibers coursing into and out of the view. (C) Photograph of sheath-core-constructed rope models for hagfish bodies: (i.) two structural components of rope: the sheath (or skin) and the core (or body core musculature). (ii.)(iii.) Two models of varying sheath tautness. Model ii. possesses a slacker sheath than model iii., which can result from covering a shorter core with an equal amount of mantle. Note the increased stiffness in tauter rope model iii. (iv.) Two rope models of equal sheath tautness and core length, assembled in a figure-eight knot (top) and trefoil knot (bottom).

The total thickness of Pacific hagfish skins collected from the head and tail regions spanned a larger range (270–900 μm) than did the skins from the head and tail regions of penpoint gunnells (440–720 μm) and sea lamprey (160–200 μm) (Table 3). The mean total thickness of hagfish skin was

$667.1 \pm 20.2 \mu\text{m}$ at the head, $464.3 \pm 25.0 \mu\text{m}$ at the tail, and $517.8 \pm 18.1 \mu\text{m}$ at the ventral surface beneath the feeding apparatus (Fig. 4A). Mean subdermal thickness at the head was $518.6 \pm 18.6 \mu\text{m}$, compared with $317.3 \pm 25.2 \mu\text{m}$ and $356.5 \pm 25.2 \mu\text{m}$ at the tail and ventral

Table 3

Total skin thickness of jawless fishes, cartilaginous fishes, and bony fishes

Species; family	Total thickness (μm)	Source
<i>Eptatretus stoutii</i> ; Myxinidae	270–900	Present study
<i>Petromyzon marinus</i> ; Petromyzontidae	160–200	Present study
<i>Apodichthys flavidus</i> ; Pholidae	440–720	Present study
<i>Anguilla rostrata</i> ; Anguillidae	150–530	Hebrank, 1980
<i>Leiostomus xanthurus</i> ; Sciaenidae	220–300	Hebrank and Hebrank, 1986
<i>Katsuwonus pelamis</i> ; Scombridae	280–350	Hebrank and Hebrank, 1986
<i>Scoliodon laticaudus</i> ; Carcharhinidae	1500–2000	Naresh <i>et al.</i> , 1997
<i>Gymnothorax griseus</i> ^a ; Heterocongridae	450–1150	Fishelson, 1996
<i>Gymnothorax nudivomer</i> ^b ; Muraenidae	200–400	Fishelson, 1996
<i>Gymnothorax undulatus</i> ; Muraenidae	400–2100	Fishelson, 1996
<i>Gymnothorax hepaticus</i> ; Muraenidae	160–340	Fishelson, 1996
<i>Gorgasia sillneri</i> ; Muraenidae	110–1320	Fishelson, 1996
<i>Rhinomuraena quaesita</i> ^c ; Muraenidae	180–480	Fishelson, 1996

Data are presented in ranges from minimum to maximum values.

^a Previously known as *Siderea grisea*.

^b Previously known as *Lycodontis nudivomer*.

^c Previously known as *Rhinomuraena ambonensis*.

regions, respectively; however, these means did not differ significantly. Thickness of the dermis ($148.4 \pm 4.27 \mu\text{m}$ at the head, $147.0 \pm 9.28 \mu\text{m}$ at the tail, and $161.3 \pm 7.30 \mu\text{m}$ at the ventral surface) remained conserved across all parts of the hagfish body (Fig. 4A).

Discussion

Material properties

Loose-fitting hagfish skins are comparable in strength and stiffness to the tight-fitting skins of bony fishes, cartilaginous fishes, and lamprey (Fig. 3C). As mentioned earlier, hagfish skin is anisotropic. However, the patterns by which hagfish skin differentially responds to longitudinally and circumferentially directed loads contrasts with published values for tight-fitting fish skins. Hagfish skin is stiffer along the animal's longitudinal axis than its circumferential axis. The anisotropy observed in skins hypothesized to function like external tendons, such as those from American eels (Hebrank, 1980) and some sharks (Wainwright *et al.*, 1978; Naresh *et al.*, 1997), in which the skin is twice as stiff in the circumferential direction than in the longitudinal direction, is characteristic of pressurized cylinder walls. Skin samples of penpoint gunnels from our study demonstrated the same mechanical responses to circumferentially and longitudinally directed loads as did published data gathered from similar testing of other taut fish skins (Fig. 3C). Even fish skins that do not function like external tendons (*e.g.*, Norfolk spot and skipjack tuna) exhibit higher stiffness along the circumferential axis than the longitudinal axis when strained uniaxially (Hebrank and Hebrank, 1986). It is worth noting that newly metamorphosed forms of sea

lamprey possess skins that are quite stiff with respect to longitudinal strains (Fig. 3A, Table 1).

The anisotropy that we observed in the skin samples of the Pacific hagfish supports the idea that hagfish could benefit from skins that are less resistant to circumferentially directed tensile stresses and strains, considering the amount of torsion experienced by the knotting body. Thus, the knotting movements of hagfish could be facilitated with slack skins, which are more compliant in the circumferential axis. These results show that hagfish integument, as a considerably strong and stiff covering, could promote successful knotting movements. However, the skin is functionally irrelevant to steady swimming, given its slackness and its minimal influence on cyclic, flexural movements of the whole body. Results from dynamic testing experiments performed on Atlantic hagfish bodies set to oscillate at biologically relevant speeds have suggested that these animals could swim without their skin (Long *et al.*, 2002b). Instead of the skin, subcutaneous sinus, and body core muscles, it is the notochord that accounts for approximately 70% of the animal's whole-body stiffness (Long *et al.*, 2002b).

With respect to each direction of applied tension (longitudinal or circumferential), the skins of Pacific hagfish and penpoint gunnels appear to be stiffer and stronger near the tail than near the head (Fig. 3A); however, this possibility is at odds with our statistical results (Table 1). Although these differences were statistically insignificant, there is potential biological significance in the numbers we gathered. The tail regions of swimming, elongate animals are the body segments that experience the greatest curvatures, axial strains, and body wave amplitudes (Gillis, 1996). Furthermore, knot

formation is always initiated at the tail of a hagfish, where the body experiences the greatest curvatures and strains.

Puncture resistance

Hagfishes would certainly benefit from possessing puncture-resistant skin, as they lack dermal scales and occasionally encounter predators. The thick skins of eels have been theorized to be useful for transmitting forces to tendon-like skins while protecting the body from abrasive interactions with the substrates they move against and sometimes burrow into (Hebrank and Hebrank, 1986; Fishelson, 1996). In contrast, ambush predatory fishes may benefit from thinner, lighter-weight skins for rapid acceleration (Webb and Skadsen, 1979). Like eel skins, shark skins are thick, and they appear to function well against biting assaults associated with courting behaviors (Hebrank and Hebrank, 1986). The comparably thick skins of Pacific hagfish could offer some resistance to puncture (Table 3); however, measurements of puncture resistance are needed. Furthermore, it is the dermal scales of many fish skins that best account for puncture resistance.

Shark skins bear thousands of rigid denticles, or placoid scales, comprised of hard materials, such as dentin and enamel, which are high in strength and stiffness (Raschi and Tabit, 1992). Individual teleost scales are highly resistant to puncture, and undergo a two-step failure process by which the stiff, outer bony layer fractures first, followed by input of an additional 50% of puncture force to induce secondary failure of the deeper collagenous layer before assaulting the dermis (Zhu *et al.*, 2012). It has been demonstrated that the scales around the punctured scale redistribute the puncture forces over a larger surface area in order to prevent injury to the softer tissue beneath the damaged scale (Vernerey and Barthelat, 2010; Zhu *et al.*, 2013). Like many scale-bearing sharks and bony fishes, most extinct, jawless fishes possessed articulating dermal bones that were suggested to be adaptations against predators (Carroll, 1988).

Wild specimens of hagfishes have been recorded avoiding predatory attacks by ram-feeding fishes, like seal sharks and conger eels, and suction-feeding fishes, such as scorpionfishes and wreckfishes (Zintzen *et al.*, 2011). The scaleless skin resists puncture and abrasive damage during contact with the predator's oral or pharyngeal teeth; then, immediately after the initial strike, the hagfish employs its slime defense mechanism, which clogs the fish predators' gills (Lim *et al.*, 2006; Fudge *et al.*, 2015). Once released from its attacker, the hagfish swims away without any apparent damage to its skin or swimming ability (Zintzen *et al.*, 2011). These observations demonstrate that hagfish skin effectively resists puncture despite lacking rigid scales, indicating that hagfishes must rely on loose-fitting skins as a softer strategy against predatory bites. Even if the skin itself were not a puncture-resistant covering, the slimy skin's

low-friction surface and its looseness could effectively impede a predator from successfully grasping the decoupled body core.

Functional morphology of hagfish skin

An enticing explanation for the puncture resistance of hagfish integument is the thickness of the skins that we recorded from the Pacific hagfish, which were comparable to the thickness of many eel skins (Table 3). However, most of the thickness of hagfish skin is comprised of the fatty subdermis (or hypodermis). The subdermis of the Pacific hagfish examined here (Fig. 4B) bears similar characteristics to the fatty tissues of the *stratum spongiosum* described in the American eel *Anguilla rostrata*, which could function in storing chemical energy for migration habits (Danos *et al.*, 2008). Therefore, it is possible that the function of this proportionately thick tissue layer in hagfish is to store energy during the long starvation periods the animals endure between feedings (*e.g.*, one year; A. J. Clark, pers. obs.). The fatty subdermis in hagfish offers very little if any resistance to mechanical stresses and strains associated with biting attacks. However, these soft-tissue layers have been thought to aid in damping physical stresses associated with burrowing movements in the snakehead murrel *Channa striata* (Mittal and Banerjee, 1975).

The extremely thin epidermal layer of the hagfish skin offers little mechanical reinforcement and puncture resistance, but it contains slime glands (Spitzer and Koch, 1998) and can absorb dissolved organic nutrients while residing in decaying carcasses (Glover *et al.*, 2011). Most of the mechanical stiffness of the skin comes from the fibrous dermis (Welsch *et al.*, 1998), which comprises less than half of the total skin thickness (Fig. 4A, B). Perhaps the most effective means for resisting puncture, before sliming, is the smooth texture and loose fit of the skin. These characteristics render the hagfish skin exceedingly difficult to grasp between a set of occluding teeth. A predator's teeth are more effective at puncturing when applied to pre-stressed, higher-friction surfaces (*e.g.*, tight-fitting, scaled skins) than when applied to a loosely suspended, lower-friction surface, such as hagfish skin.

The subcutaneous sinus also provides some protection of the body core of a hagfish. Previous experiments with oscillating body segments of Atlantic hagfish *Myxine glutinosa* indicated that the subcutaneous sinus could aid in flexural damping, even though it would impede thrust production (Long *et al.*, 2002b). This loose connection associated with the sinus may be functionally important during knotting, when axial strains could impose damaging levels of tension on the skin. In addition to reducing circulatory output requirements (Davison *et al.*, 1990), the low viscosity of the blood in the subcutaneous sinus could facilitate

knotting by reducing friction between the skin and axial muscles.

Knotting

The feeding behaviors of many fishes involve integrated movements of cranial and postcranial systems (Higham, 2007). Species with elongate, limbless bodies and small gapes often circumvent constraints imposed by this morphology by using either rotational or knotting feeding strategies when negotiating large prey. Of these, rotational feeding is the better understood method (Helfman and Clark, 1986; Measey and Herrel, 2006); there are descriptions for muraenid (Miller, 1987) and anguillid eels (Helfman and Clark, 1986), some non-anguillid teleosts (*e.g.*, *Monopterus* sp. and *Synbranchus* sp. (Liem, 1980)), and caecilians (Summers and Wake, 2005; Measey and Herrel, 2006). From our personal observations in laboratory settings, rapid rotational biting can be elicited in gunnels and pricklebacks when they are presented with large food items. The less understood knotting behaviors occur in hagfishes (Jensen, 1966; Uyeno and Clark, 2015), a pelagic sea snake *Pelamis platurus* (Pickwell, 1971), and at least six species of moray eels (Miller, 1987). Among the many integrated head-body movements used by vertebrates for handling large prey (*e.g.*, head shaking and use of forelimbs), the knotting behavior of hagfish represents an ancestral vertebrate strategy for handling oversized food items.

Myxinid knot manipulation is powered by a complex arrangement of body core musculature, which, unlike that of other basal chordates and fishes, is uniquely divided into segmented parietal and rectus muscles, both of which are overlapped by superficial, non-segmented oblique muscles (Cole, 1907; Jansen and Andersen, 1963; Vogel and Gemballa, 2000). Comprising the bulk of the body core musculature, the parietal muscle extends along the animal's longitudinal axis from behind the nasal capsule to the tail, and along the orthogonal (circumferential) axis from the dorsal midline to the slime glands; it bears longitudinally oriented fibers (Fig. 1D). Because hagfishes lack a horizontal septum, the parietal muscle is not divided into dorsal and ventral portions like the axial musculature of other fishes (Cole, 1907; Jansen and Andersen, 1963). The rectus muscle is a long, narrow band of segmented muscle extending along the ventral midline, from the ventral surface of the middle basal plate to the cloaca; it, too, possesses a longitudinal fiber orientation. The thin, oblique muscle is a superficial sheet of unsegmented muscle that overlaps the rectus and the ventral portion of the parietal muscle (Fig. 1A, D). Its obliquely arranged fibers are oriented in a caudo-ventral direction and interdigitate at the ventral midline (Cole, 1907; Jansen and Andersen, 1963). This organization of musculature resembles the derived trunk musculature in tetrapods, which involves multiple, thin

overlapping sheets of muscles comprising variable fiber orientations (Liem *et al.*, 2001). Given the derived body core musculature in hagfishes, it is clear that chordate axial musculature underwent more than a simple evolutionary transition from the serially arranged, segmented muscles in basal taxa (*e.g.*, lancelets) and most fishes, to the non-segmented, complex arrangements of overlapping oblique muscles of tetrapods.

We propose that the slack skins of hagfishes confer the flexibility required for generating and manipulating knots. Much of the biomechanical complexity of the hagfish body may be simplified using an appropriate physical model: a rope consisting of a central core (*e.g.*, axial muscles) surrounded by a braided sheath (*e.g.*, the integument) (Fig. 4C). Using this approach to characterize hagfish body construction, we see that for a given length of core, a rope's flexibility increases by the doubling of its sheath length. Increasing the length of the sheath effectively loosens its fit relative to the core, producing a rope that is passively flexible; in contrast, a tighter-fitting sheath grants the rope more flexural stiffness (Fig. 4C). In hagfish and moray eels, which use knots in feeding, these can be either figure-eight or overhand (trefoil) knots (Jensen, 1966; Miller, 1987). From a mechanical point of view, knot topology studies have shown that overhand knots bear larger stresses on key points within the knot, and are therefore weaker than figure-eight knots (Pieranski *et al.*, 2001). This finding may explain why hagfish feeding on large or tethered prey in laboratory conditions almost always employ a figure-eight knot (A. J. Clark *et al.*, pers. obs.). It is interesting to note that the thick, fatty, slimy, scaleless, and slack morphology of hagfish skins is also characteristic of the skins of moray eels. This suggests that this morphology may be beneficial for knotting movements, even though it offers little for steady swimming movements.

Acknowledgments

We want to thank Kim Penttila (California Fish and Game Commission) for organizing the collecting and shipping of hagfish specimens. Adam Summers (Friday Harbor Laboratories) provided the MTS materials testing system and, with the 2012 *FISHES* summer course, helped in the collection and husbandry of the gunnel specimens. This research was supported by funds from the College of Charleston Biology Department (awarded to AJC), a SURF grant (awarded to AMD), and a National Science Foundation grant (no. IOS-1354788 awarded to TAU and AJC).

Literature Cited

- Brainerd, E. L. 1994. Pufferfish inflation: functional morphology of postcranial structures in *Diodon holocanthus* (Tetraodontiformes). *J. Morphol.* **220**: 243–261.

- Carroll, R. L. 1988.** *Vertebrate Paleontology and Evolution*. W. H. Freeman, New York.
- Clark, A. J., and A. P. Summers. 2007.** Morphology and kinematics of feeding in hagfish: possible functional advantages of jaws. *J. Exp. Biol.* **210**: 3897–3909.
- Clark, A. J., and A. P. Summers. 2012.** Ontogenetic scaling of the morphology and biomechanics of the feeding apparatus in the Pacific hagfish *Eptatretus stoutii*. *J. Fish Biol.* **80**: 86–99.
- Clark, R. B., and J. B. Coway. 1985.** Factors controlling the change of shape of certain nemertean and turbellarian worms. *J. Exp. Biol.* **35**: 731–748.
- Cole, F. J. 1907.** A monograph of the general morphology of the myxinoïd fishes, based on a study of Myxine. Part 2. The anatomy of the muscles. *Trans. R. Soc. Edinb.* **45**: 683–757.
- Danos, N., N. Fisch, and S. Gemballa. 2008.** The musculotendinous system of an anguilliform swimmer: muscles, myosepta, dermis, and their interconnections in *Anguilla rostrata*. *J. Morphol.* **269**: 29–44.
- Davison, W., J. Baldwin, P. S. Davie, M. E. Forster, and G. H. Satchell. 1990.** Exhausting exercise in the hagfish, *Eptatretus cirrhatus*: the anaerobic potential and the appearance of lactic acid in the blood. *Comp. Biochem. Physiol. Part A Physiol.* **95**: 585–589.
- Evans, D. H., and A. C. Harrie. 2001.** Vasoactivity of the ventral aorta of the American eel (*Anguilla rostrata*), Atlantic hagfish (*Myxine glutinosa*), and sea lamprey (*Petromyzon marinus*). *J. Exp. Biol.* **289**: 273–284.
- Fishelson, L. 1996.** Skin morphology and cytology in marine eels adapted to different lifestyles. *Anat. Rec.* **246**: 15–29.
- Forster, M. E. 1998.** Cardiovascular function in hagfishes. Pp. 237–258 in *The Biology of Hagfishes*, J. M. Jørgensen, J. P. Lomholt, R. E. Weber, and H. Malte, eds. Chapman & Hall, London.
- Fudge, D. S., S. Schorno, and S. Ferraro. 2015.** Physiology, biomechanics, and biomimetics of hagfish slime. *Annu. Rev. Biochem.* **84**: 947–967.
- Fujii, R. 1968.** Fine structure of the collagenous lamella underlying the epidermis of the goby, *Chasmichthys gulosus*. *Annot. Zool. Jpn.* **41**: 95–106.
- Gemballa, S., and K. Treiber. 2003.** Cruising specialists and accelerators: are different types of fish locomotion driven by differently structured myosepta? *Zoology* **106**: 203–222.
- Gemballa, S., and F. Vogel. 2002.** Spatial arrangement of white muscle fibers and myoseptal tendons in fishes. *Comp. Biochem. Physiol. Part A Mol. Integr. Physiol.* **133**: 1013–1037.
- Gillis, G. B. 1996.** Undulatory locomotion in elongate aquatic vertebrates: anguilliform swimming since Sir James Gray. *Am. Zool.* **36**: 656–665.
- Glover, C. N., C. Bucking, and C. M. Wood. 2011.** Adaptations to *in situ* feeding: novel nutrient acquisition pathways in an ancient vertebrate. *Proc. R. Soc. Lond. B Biol. Sci.* **278**: 3096–3101.
- Hebrank, M. R. 1980.** Mechanical properties and locomotor functions of eel skin. *Biol. Bull.* **158**: 58–68.
- Hebrank, M. R., and J. H. Hebrank. 1986.** The mechanics of fish skin: lack of an “external tendon” role in two teleosts. *Biol. Bull.* **171**: 236–247.
- Helfman, G. S., and J. B. Clark. 1986.** Rotational feeding: overcoming gape-limited foraging in anguillid eels. *Copeia* **1986**: 679–685.
- Higham, T. E. 2007.** The integration of locomotion and prey capture in vertebrates: morphology, behavior, and performance. *Integr. Comp. Biol.* **47**: 82–95.
- Jansen, J. K., and P. Andersen. 1963.** Anatomy and physiology of the skeletal muscles. Pp. 161–194 in *The Biology of Myxine*, A. Brodal, R. Fänge, and J. Jansen, eds. Universitetsforlaget, Oslo.
- Jensen, D. 1966.** The hagfish. *Sci. Am.* **214**: 82–90.
- Liem, K. F. 1980.** Acquisition of energy by teleosts: adaptive mechanisms and evolutionary patterns. Pp. 299–334 in *Environmental Physiology of Fishes*, M. A. Ali, ed. Springer, New York.
- Liem, K. F., W. E. Bemis, J. W. F. Walker, and L. Grande. 2001.** *Functional Anatomy of the Vertebrates: An Evolutionary Perspective*, 3rd ed. Brooks/Cole Publishing, Pacific Grove, CA.
- Lim, J., D. S. Fudge, N. Levy, and J. M. Gosline. 2006.** Hagfish slime ecomechanics: testing the gill-clogging hypothesis. *J. Exp. Biol.* **209**: 702–710.
- Long, J. H., Jr., M. E. Hale, M. J. McHenry, and M. W. Westneat. 1996.** Functions of fish skin: flexural stiffness and steady swimming of longnose gar, *Lepisosteus osseus*. *J. Exp. Biol.* **199**: 2139–2151.
- Long, J. H., Jr., B. Adcock, and R. G. Root. 2002a.** Force transmission via axial tendons in undulating fish: a dynamic analysis. *Comp. Biochem. Physiol. Part A Mol. Integr. Physiol.* **133**: 911–929.
- Long, J. H., Jr., M. Koob-Emunds, B. Sinwell, and T. J. Koob. 2002b.** The notochord of hagfish *Myxine glutinosa*: visco-elastic properties and mechanical functions during steady swimming. *J. Exp. Biol.* **205**: 3819–3831.
- McDonald, D. G., V. Cavdek, L. Calvert, and C. L. Milligan. 1991.** Acid-base regulation in the Atlantic hagfish *Myxine glutinosa*. *J. Exp. Biol.* **161**: 201–215.
- Measey, G. J., and A. Herrel. 2006.** Rotational feeding in caecilians: putting a spin on the evolution of cranial design. *Biol. Lett.* **2**: 485–487.
- Miller, T. J. 1987.** Knotting: a previously undescribed feeding behavior in muraenid eels. *Copeia* **1987**: 1055–1057.
- Mittal, A. K., and T. K. Banerjee. 1975.** Histochemistry and the structure of the skin of a murrel, *Channa striata* (Bloch, 1797) (Channiformes, Channidae). I. Epidermis. *Can. J. Zool.* **53**: 833–843.
- Motta, P. J. 1977.** Anatomy and functional morphology of dermal collagen fibers in sharks. *Copeia* **1977**: 454–464.
- Müller, U. K., and J. L. Van Leeuwen. 2006.** Undulatory fish swimming: from muscles to flow. *Fish Fish.* **7**: 84–103.
- Naresh, M. D., V. Arumugam, and R. Sanjeevi. 1997.** Mechanical behaviour of shark skin. *J. Biosci.* **22**: 431–437.
- Pickwell, G. V. 1971.** Knotting and coiling behavior in the pelagic sea snake *Pelamis platurus* (L.). *Copeia* **1971**: 348–350.
- Pieranski, P., S. Kasas, G. Dietler, J. Dubochet, and A. Stasiak. 2001.** Localization of breakage points in knotted strings. *New J. Phys.* **3**: 10.1–10.13.
- Raschi, W., and C. Tabit. 1992.** Functional aspects of placoid scales: a review and update. *Aust. J. Mar. Freshw. Res.* **43**: 123–147.
- Spitzer, R. H., and E. A. Koch. 1998.** Hagfish skin and slime glands. Pp. 109–132 in *The Biology of Hagfishes*, J. M. Jørgensen, J. P. Lomholt, R. E. Weber, and H. Malte, eds. Chapman & Hall, London.
- Summers, A. P., and J. H. Long, Jr. 2006.** Skin and bones, sinew and gristle: the mechanical behavior of fish skeletal tissues. Pp. 141–177 in *Fish Biomechanics*, R. E. Shadwick and G. V. Lauder, eds. Elsevier, Amsterdam.
- Summers, A. P., and M. H. Wake. 2005.** The retroarticular process, streptostyly and the caecilian jaw closing system. *Zoology* **108**: 307–315.
- Urist, M. R. 1963.** The regulation of calcium and other ions in the serums of hagfish and lampreys. *Ann. N. Y. Acad. Sci.* **109**: 294–311.
- Uyeno, T. A., and A. J. Clark. 2015.** Muscle articulations: flexible jaw joints made of soft tissues. *Integr. Comp. Biol.* **55**: 193–204.
- Vernerey, F. J., and F. Barthelat. 2010.** On the mechanics of fishscale structures. *Int. J. Solids Struct.* **47**: 2268–2275.
- Vogel, F., and S. Gemballa. 2000.** Locomotory design of ‘cyclostome’ fishes: spatial arrangement and architecture of myosepta and lamellae. *Acta Zool.* **81**: 267–283.
- Vogel, S. 1994.** *Life in Moving Fluids: the Physical Biology of Flow*. Princeton University Press, Princeton.

- Wainwright, S. A., F. Vosburgh, and J. H. Hebrank. 1978.** Shark skin: function in locomotion. *Science* **202**: 747–749.
- Webb, P. W., and J. M. Skadsen. 1979.** Reduced skin mass: an adaptation for acceleration in some teleost fishes. *Can. J. Zool.* **57**: 1570–1575.
- Welsch, U., S. Büchl, and R. Erlinger. 1998.** The dermis. Pp. 133–142 in *The Biology of Hagfishes*, J. M. Jørgensen, J. M. Lomholt, R. E. Weber and H. Malte, eds. Chapman & Hall, London.
- Zhu, D., C. F. Ortega, R. Motamedi, L. Szewciw, F. Vernerey, and F. Barthelat. 2012.** Structure and mechanical performance of a “modern” fish scale. *Adv. Eng. Mater.* **14**: B185–B194.
- Zhu, D., L. Szewciw, F. Vernerey, and F. Barthelat. 2013.** Puncture resistance of the scaled skin from striped bass: collective mechanisms and inspiration for new flexible armor designs. *J. Mech. Behav. Biomed. Mater.* **24**: 30–40.
- Zintzen, V., C. D. Roberts, M. J. Anderson, A. L. Stewart, C. D. Struthers, and E. S. Harvey. 2011.** Hagfish predatory behaviour and slime defence mechanism. *Sci. Rep.* **1**: 1–6.